Journal of Medicinal Chemistry Article

J. Med. Chem. **2010,** *53,* 745–751 **745**
DOI: 10.1021/jm901296p

Probing *Torpedo californica* Acetylcholinesterase Catalytic Gorge with Two Novel Bis-functional Galanthamine Derivatives†

Cecilia Bartolucci,‡ Lars A. Haller,§ Ulrich Jordis,∥ Gregor Fels,§ and Doriano Lamba*,⊥

‡*Istituto di Cristallografia, Consiglio Nazionale delle Ricerche, Area della Ricerca di Roma, P.O. Box 10, I-00016 Monterotondo Stazione (Roma), Italy,* §*Department of Chemistry, University of Paderborn, Warburger Strasse 100, D-33098 Paderborn, Germany,* ∥*Vienna University of Technology, Institute for Organic Chemistry, Getreidemarkt 9, A-1060 Wien, Austria, and* ⊥*Istituto di Cristallografia, Consiglio Nazionale delle Ricerche, UOS di Trieste, Area Science Park, Basovizza S.S 14 Km 163.5, I-34149 Trieste, Italy*

Received July 23, 2009

N-Piperidinopropyl-galanthamine (**2**) and *N*-saccharinohexyl-galanthamine (**3**) were used to investigate interaction sites along the active site gorge of *Torpedo californica* actylcholinesterase (*Tc*AChE). The crystal structure of *Tc*AChE-**2** solved at 2.3 Å showed that the *N*-piperidinopropyl group in **2** is not stretched along the gorge but is folded over the galanthamine moiety. This result was unexpected because the three carbon alkyl chain is just long enough for the bulky piperidine group to be placed above the bottleneck (Tyr121, Phe330) midway down the gorge. The crystal structure of *Tc*AChE-**3** at 2.2 Å confirmed that a dual interaction with the sites at the bottom, and at the entrance of the gorge, enhances inhibitory activity: a chain of six carbon atoms has, in this class of derivatives, the correct length for optimal interactions with the peripheral anionic site (PAS).

Introduction

With the increase of the elderly population and considering that Alzheimer's disease (AD[a]) is thought to be the leading cause in senile dementia, the development of an effective therapeutic treatment of this syndrome is of primary importance and would have a great social impact because AD causes impairment of functioning in everyday life. Unfortunately, the real cause of the disease is still unknown and this makes a systematic research for new drugs very difficult. It has been shown however that, associated with AD, is a loss of the cholinergic response due to reduced activity of choline acetyltransferase, the enzyme responsible for the synthesis of acetylcholine[1] (ACh) as well as reduced levels of nicotinic ACh receptors.[2] Hence the rationale behind the current approach of cholinergic therapeutics used in the treatment of AD aims at targeting the inhibition of acetylcholinesterase (AChE) in the brain, which results in an elevation of the ACh concentration and therefore in the activation of the cholinergic transmission as well as allosterically potentiating ligands that enhance nicotinic receptors activation through nicotinic agonists.[3,4] Many years after the approval of symptomatic drugs such as tacrine,[5] donepezil,[6] rivastigmine,[7] and galanthamine (**1**),[8] the improvement of old and the development of new drugs targeting the cholinergic system is still pursued both by pharmaceutical companies as well as many research groups.

Galanthamine (**1**) is a natural alkaloid belonging to the Amaryllidaceae family and is among the very few ligands showing a dual mechanism of action, reversibly inhibiting AChE as well as enhancing the intrinsic action of ACh on nicotinic receptors by allosteric potentiation.[3,4] Hence the synthesis of new derivatives of **1** and their evaluation as anti-Alzheimer drugs continues in the hope of finding a compound showing better pharmacokinetic as well as pharmacodynamic characteristics.[8−11]

In this context, we determined the X-ray crystal structure of AChE from *Torpedo californica, Tc*AChE, complexed with two new galanthamine derivatives, chosen among those developed in the laboratory of Jordis et al.,[12] *N*-piperidinopropyl-galanthamine hydrobromide ((4a*S*,6*R*,8a*S*)-4a,5,9,10,11,12-hexahydro-3-methoxy-11-[3-(1-piperidinyl)propyl]-6*H*-benzofuro[3a,3,2-*ef*][2] benzazepin-6-ol, dihydrobromide dihydrate (**2**) and *N*-saccharinohexyl-galanthamine fumarate (2-[6-[(4a*S*,6*R*,8a*S*)-4a,5,9,10-tetrahydro-6-hydroxy-3-methoxy-6*H*-benzofuro[3a,3,2-*ef*][2]benzazepin-11(12*H*)-yl]hexyl]-1,2-benzisothiazol-3(2*H*)-one 1,1-dioxide mono fumarate (**3**) (Scheme 1).

A characteristic feature of *Tc*AChE is that the catalytic triad, typical of a serine hydrolase and formed by residues Ser200, His440, and Glu327, is placed almost at the bottom of a narrow, approximately 20 Å deep gorge, which is lined by conserved aromatic residues making up about 70% of the gorge surface. In particular, Trp84 is responsible for the cation−π interactions with the quaternary group of the substrate, while Tyr70 and Trp279 contribute to the peripheral anionic site (PAS) at the entrance of the gorge and serve as molecular traffic switch for the substrates toward the active site. Trp233, Phe288, and Phe290 constitute the acyl pocket, which determines the specificity for ACh. Halfway down the gorge, there is a bottleneck formed by Tyr121 and Phe330. At

†Atomic coordinates and structure factor amplitudes of the *Tc*AChE-**2** and *Tc*AChE-**3** complexes have been deposited in the Brookhaven Protein Data Bank under PDB ID codes 3I6M and 3I6Z, respectively.

*To whom correspondence should be addressed. Phone: +39-040-3758514. Fax: +39-040-9221126. E-mail: doriano.lamba@ts.ic.cnr.it.

[a]Abbreviations: AD, Alzheimer's disease; ACh, acetylcholine; AChE, acetylcholinesterase; *Tc*, *Torpedo californica*; PAS, peripheral anionic site; N-PP, *N*-piperidinopropyl.

Published on Web 12/21/2009

Scheme 1. Synthesis of Galanthamine Derivatives **2** and **3** from Norgalanthamine **4**[a]

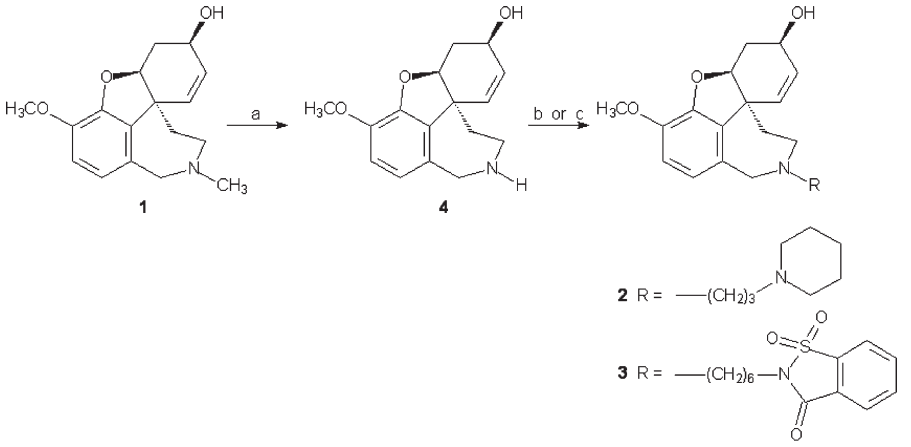

[a] Reagents and conditions: (a) (1) mCPBA, CH_2CL_2; (2) $FeSO_4$, MeOH, (b) *N*-(3-chloropropyl)piperidine, NaI, K_2CO_3, acetone; (c) *N*-(ω-bromohexyl)saccharin, $EtN(i\text{-}Pr)_2$, $CHCl_3$.

this point, the cross-section can be as narrow as 5 Å. While Tyr121 is almost fixed in all crystal structures, Phe330, acting as a swinging gate, is quite flexible and was found to adopt different side-chain conformations in order to interact through $\pi-\pi$ stacking or cation$-\pi$ interaction with the bound ligands.

Both compounds chosen for the present study are substituted at the nitrogen atom of the tetrahydroazepine ring of galanthamine, which structure–activity relationship studies[13−15] showed to result in improved inhibitory activity, however, they differ in the length of the alkyl chain, as well as in the substituent at the end of the chain. With the elucidation of the structure of the complex with **2**, we expected to investigate the interactions of the piperidinium ring with the amino acids present in the middle of the gorge. **2** shows an activity approximately six times higher than **1**, having an IC_{50} value of 0.35 μM on recombinant human brain AChE compared to a value of 2.10 μM shown by **1**. Previous docking studies[16] revealed that an alkyl spacer with just three carbon atoms is in fact too short to allow an interaction of the piperidinium moiety with the amino acids belonging to the PAS; it should however be long enough to enable an interaction of the piperidinium ring with the aromatic residues of Tyr121 and Phe330, the swinging gate, halfway down the gorge. The aim of the determination of the structure of *Tc*AChE in complex with compound **3** was to confirm the assumption that a better inhibitory activity is achieved by those compounds, which interact with both the active site at the bottom of the gorge and the PAS. In particular, the bivalent galanthamine having a phtalimido moiety as substituent[17] shows a higher activity. Furthermore, we wanted to explore the role of the added sulphonyl functional group on the indanone ring, not present in any other long chain derivatives, which could unveil a new interacting site and have an additional stabilizing role (hydrogen bonding donor–acceptor), through a direct and/or a water mediated hydrogen-bonding network. In fact, the activity of **3**, measured on recombinant human brain AChE (IC_{50} 0.05 μM) is more than 40 times higher than the activity of **1** (IC_{50} 2.10 μM).

Results and Discussion

Synthesis of 2 and 3. Compounds **2** and **3** were prepared according to a general synthetic procedure shown in Scheme 1 using nor-galanthamine (**4**) as starting material, which can be derived from **1** by selective *N*-demethylation via a nonclassical Polonovski reaction.[18,19] Treatment of **4** with *N*-(3-chloropropyl)piperidine in the presence of potassium carbonate and sodium iodide in acetone for three days under refluxing conditions gave rise to compound **2** in 75% yield after purification by flash chromatography. The free base was converted to the dihydrobromide dihydrate in 63% yield by reaction with HBr in an ethanol/diethyl ether mixture. Accordingly, compound **3** was synthesized in 71% yield by refluxing **4** in chloroform for 24 h with *N*-(ω-bromohexyl)-saccharin[20] as alkylating agent in the presence of *N*-ethyldiisopropylamine. An ethanol solution of compound **3** as free base and fumaric acid was slowly added to diethyl ether to give a 76% yield of the corresponding fumarate. Purity of the synthesized compounds was better than 95%, as evidenced by elemental analysis outlined in Materials and Methods.

Crystallography

Compound 2. The X-ray crystal structure of *Tc*AChE in complex with **2** was determined at 2.3 Å resolution. It reveals that the galanthamine moiety positions itself at the bottom of the active site gorge in the same way shown by **1**, preserving the main interactions.[21,22] The hydroxyl oxygen is engaged in a hydrogen bond with the water molecule W547 (2.8 Å), which is firmly bound to Ser200 (2.6 Å) and to the oxyanion hole residues Gly118 (2.7 Å) and Gly119 (2.8 Å) (see Figure 1A). The cyclohexene ring stacks against the π system of the indole ring of Trp84 via a $\pi-\pi$ interaction.

The structure of the *Tc*AChE-**2** complex also clearly, though unpredictably, shows that the piperidinium moiety is folded over the tetrahydroazepine ring (Figure 2A) and that this conformation is stabilized by interactions between the protonated nitrogen atom of the piperidine ring and the free electron lone pair of the nitrogen belonging to the tetrahydroazepine ring (2.9 Å). In fact, because the pH of the soaking solution is 6.0 (see Material and Methods), the nitrogen of the piperidine ring is the one likely to be protonated (pK_a = 11.25) with respect to the other nitrogen atom (pK_a = 8.33).[23] Furthermore, the piperidinium ring is accommodated within a hydrophobic pocket formed by Phe330, Phe331, and Tyr334, the distances of the centroids of the rings being 3.9, 3.8, and 4.0 Å, respectively. The seven-membered tetrahydroazepine ring, as in the *Tc*AChE-**1** (PDB ID 1QTI[21]) complex, adopts a chair conformation with the N-PP moiety in an equatorial orientation, which

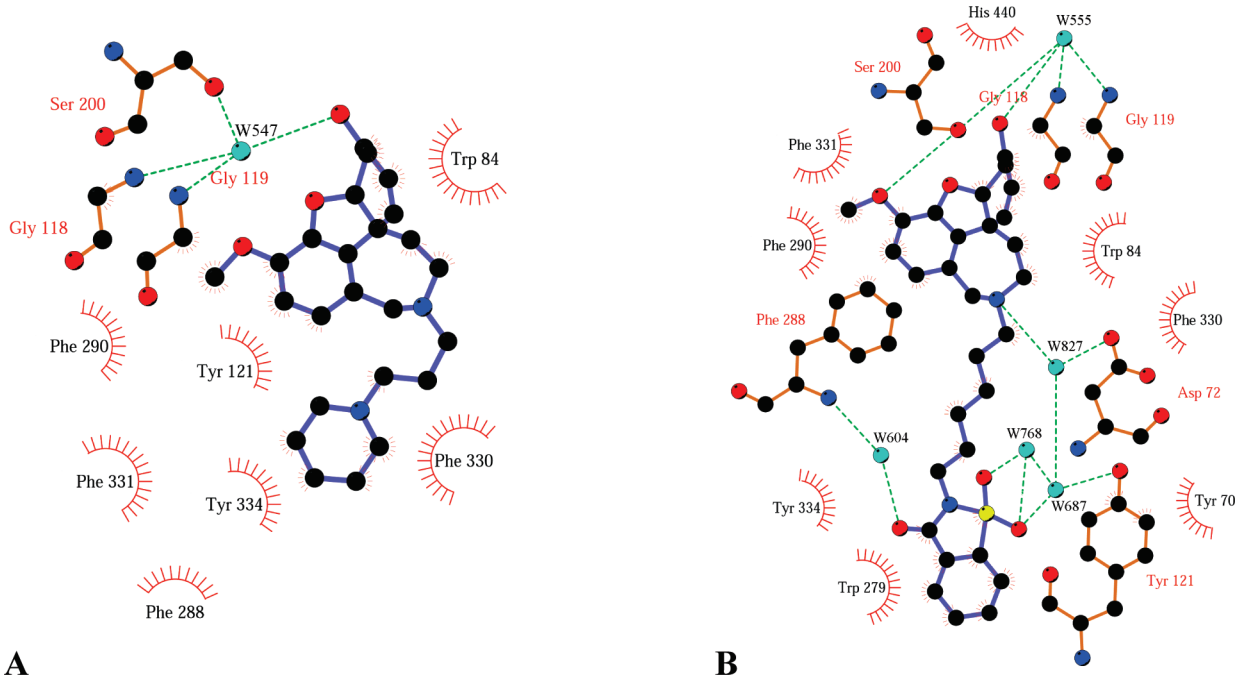

Figure 1. Ligplot[45] representations of the interactions of **2** and **3** with *Tc*AChE. (A) Interactions in the crystal structure of the *Tc*AChE-**2** complex. (B) Interactions in the crystal structure of the *Tc*AChE-**3** complex.

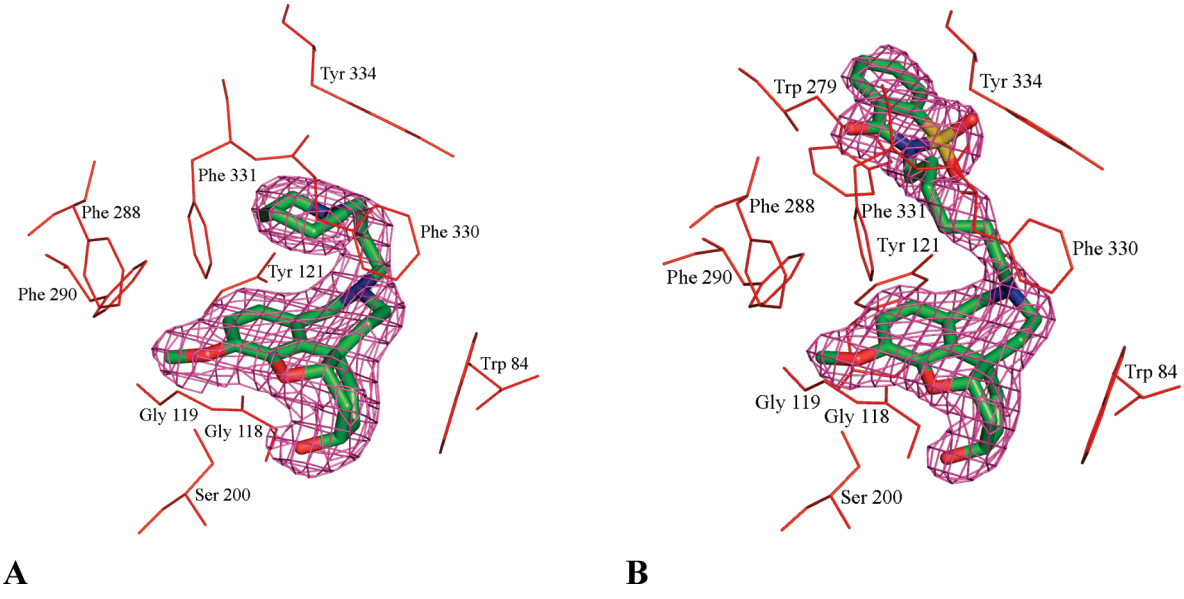

Figure 2. Close-up view of the active-site gorge area in the crystal structures of *Tc*AChE in complex with **2** (A) and **3** (B). **2** and **3** are displayed as sticks, with carbon, oxygen, nitrogen, and sulfur atoms colored green, red, blue, and yellow, respectively, and the selected *Tc*AChE residues are in red. The $2F_o - F_c$ σA-weighted electron density maps, carved around compounds **2** and **3**, are contoured at 1.0 σ.

was also predicted by docking.[16] The unexpected result was to find the alkyl chain in a folded conformation, and not fully extended, along the gorge, as anticipated in a previous docking study[16] and analogously to what observed in the crystal structures of *Tc*AChE in complex with long-chain inhibitors, such as decamethonium,[24] donepezil,[25] and MF268.[26] The piperidinium moiety is hence positioned over the tetrahydroazepine ring and the alkyl chain folded like a scorpion tail. A substituent with a three carbon alkyl chain is just long enough to allow the bulky ring to place itself beyond the constriction present midway down the gorge and constituted by Phe330 and Tyr121 (Figure 3). In the observed folded state, the piperidinium ring is further stabilized by interactions with the hydrophobic pocket formed by the aromatic residues Phe330, Phe331, and Tyr334.

The X-ray crystal structure of the *Tc*AChE-**2** complex at 2.3 Å resolution does not allow to unequivocally establish the orientation of the piperidinium ring because both rotamers, differing from one another by a 180° rotation of the single bond between the piperidino nitrogen and the neighboring methylene group of the propyl chain, fit equally well into the $2F_o - F_c$ electron density map. Furthermore, the analysis of the average temperature factors of the ligand shows that the *N*-alkyl chain-spacer (55.6 Å^2), as well as the piperidinium ring (50.9 Å^2), are highly flexible compared to the rigid galanthamine moiety (35.3 Å^2).

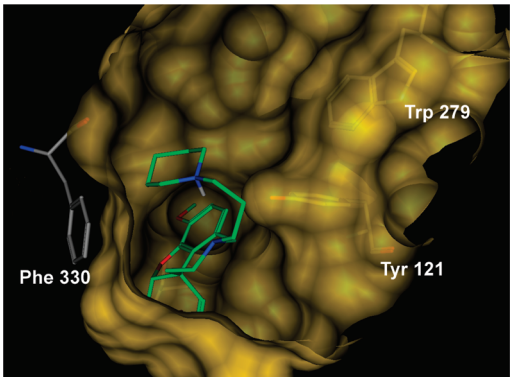

Figure 3. The piperidine ring of **2** is, in the crystal structure of the *Tc*AChE-**2** complex, beyond the bottleneck formed by Tyr121 and Phe330, which is found in the "open-gate" conformation.

With the assumption that **2** binds as a protonated ligand to *Tc*AChE,[23] we employed computational molecular modeling tools in order to select the most energetically favored piperidinium ring orientation using the QXP-Flo multistep docking procedure.[27] The results indicated that the most probable orientation of the piperidinium ring is the one in which the proton of the nitrogen faces the tetrahydroazepine ring. We hence adopted this orientation, in which the proton acts like a tether that keeps the N-PP group folded over the galanthamine moiety like a scorpion tail, in all X-ray crystallographic refinement steps.

Compound 3. The X-ray crystal structure of *Tc*AChE in complex with **3** was determined at 2.2 Å resolution. There is an overall similarity between the positioning of the two galanthamine ring systems in the crystal structures of *Tc*AChE-**3** and *Tc*AChE-**1** complexes.[21,22] At pH 6.0 (see Materials and Methods), the nitrogen of the tetrahydroazepine ring is protonated and allows an interaction, mediated through the water molecule W827, with Asp72. W827 is hydrogen-bonded to the protonated nitrogen (2.6 Å) and to the $O^{\delta 2}$ of Asp72 (2.7 Å), respectively (see Figure 1B).

As predicted by docking,[27] the hexamethylene spacer is extended along the gorge (Figure 2B) and the saccharino moiety interacts with the PAS through stacking with Trp279, the distance between the centroids of the π-system of Trp279 and the saccharino ring being 3.7 Å. The orientation of the saccharino group is further stabilized, mainly through interactions with protein main chain and/or side chain residues mediated by water molecules. In particular, the carbonyl oxygen interacts with W604 (2.9 Å), which is at a distance of 2.8 Å from the main chain nitrogen of Phe288. The sulfonic group is surrounded by a net of water molecules: one of the two oxygen atoms is at 2.9 Å from W768 and at 2.7 Å from W687; W687 also interacts with W827 (2.6 Å), W768 (3.1 Å), and with the hydroxyl O^{η} of Tyr121 (2.8 Å). Furthermore, W768 is at 2.7 Å from the second oxygen atom of the sulfonic group (see Figure 1B).

As observed in the previous structures of *Tc*AChE complexed both with **1** as well as with **2**, also in this structure, the tetrahydroazepine ring adopts a chair conformation. However, while in the former structures the orientation of the alkyl group is equatorial, as it is clearly visible from the $2F_o - F_c$ electron density map (Figure 2B), in the latter it is axial. This had been correctly predicted by previous docking studies.[28] Theoretical gas phase calculations[29] showed that the nitrogen inversion barrier in the neutral as well as in the protonated galanthamine is very low (5.3−6.8 kcal mol^{-1}), allowing the coexistence of both conformers until other factors in the local environment shift the balance toward one conformation. Docking studies predicted also that the alkyl chain would extend toward Trp279 at the PAS.[28] Six carbon atoms seem indeed to be required to allow a classical $\pi-\pi$ interaction between the saccharino group and Trp279. A similar interaction had already been observed in the complex of *Tc*AChE with a derivative of the iminium salt of galanthamine in which a phthalimido moiety is attached via an 8-carbon alkyl linker.[17]

Conclusions

In the screening process for new drugs showing a better pharmacokinetic as well as pharmacodynamic profile, the determination of the X-ray crystal structure cannot be used routinely as characterization method for all candidate lead compounds because it is a time-consuming procedure. The present paper however shows how important structural information can be gained through the determination of the X-ray crystal structures of complexes with derivatives carefully selected among several others. The structure determination of the complex of *Tc*AChE with **2** showed that the assumption made that galanthamine derivatives with long chain substituents would bind to the enzyme in the open gate conformation, allowing the chain to extend into the gorge toward the PAS, was not correct.[16] This assumption was based on the previously solved structures of *Tc*AChE in complex with long chain inhibitors such as decamethonium (PDB ID 1ACL),[24] donepezil (PDB ID 1EVE),[25] and MF268 (PDB ID 1OCE)[26] as well as on previous docking results.[16] Furthermore, comparisons among the published crystal structures of various *Tc*AChE complexes show that Phe330 is the only site of real conformational flexibility in contrast to the relative rigidity of the other side chains lining the gorge.[30,31] The *Tc*AChE-**2** crystal structure clearly shows that the swinging gate is in an open position analogously to what was observed in the *Tc*AChE-**1** complex[21] and differs from the closed position found in the *Tc*AChE-tacrine complex (PDB ID 1ACJ)[24] as well as from the half-open conformation found in the *Tc*AChE-edrophonium complex (PDB ID 2ACK).[32] We hence observe the three carbon *N*-alkyl chain winding up in such a way that allows the piperidine ring to be oriented toward the tetrahydroazepine ring so that a proton is shared between the two nitrogen atoms.

Finding the alkyl chain in a folded rather than in an extended conformation is an additional fact in favor of the assumption that the galanthamine derivative is bound in the protonated form because this form stabilizes the interaction between the piperidinium and the tetrahydroazepine rings.

The structure determination of the *Tc*AChE-**3** complex confirms that an alkyl chain of six carbon atoms is, in this class of galanthamine derivatives, of the correct length for optimal interaction with the residues of the PAS. The higher inhibitory activity shown by this compound can be hence attributed to a dual interaction with the active site at the bottom of the gorge as well as the site at the entrance of the gorge itself, further enhanced by hydrophobic interactions between the alkyl chain and residues lining the gorge. A comparison of the *Tc*AChE-complexes with **2**, **3**, and the bivalent galanthaminium derivative (1W4L)[17] demonstrates the importance of the PAS for enhanced binding of a ligand inside the gorge (Figure 4). The centroid of the benzene ring of

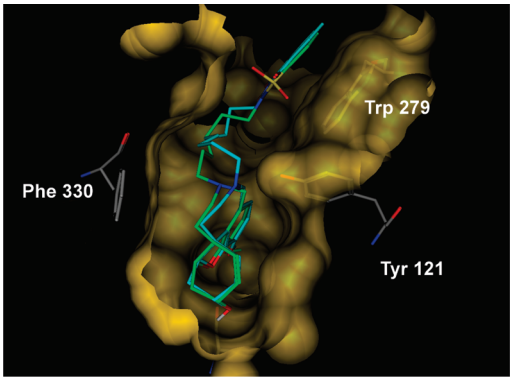

Figure 4. Overlay of *Tc*AChE-**3** crystal structure (green) on that of *Tc*AChE in complex with the *N*-phthalimido galanthamine iminium derivative (cyan).[18]

Trp279 nicely stacks against the benzene ring of the benzosulfimido moiety of **3** at a distance of 3.6 Å.

The results described for *Tc*AChE in complex with **2** and **3** show the validity of crystallographic structure determination at certain milestones along the elucidation of an enzymatic process or the development of interacting inhibitory drugs based on molecular modeling studies. It is true however that X-ray crystallography provides a time and ensemble averaged picture of the 3D structure of a protein whereas, in many cases, conformational flexibility is required for ligand binding or in catalytic reactions. A combined approach of computationally assisted structure analysis and structure elucidation by X-ray crystallography could direct the rational design of new inhibitors and the elucidation of molecular determinants in enzyme inhibition.

Materials and Methods

IC_{50}-values of **1**, **2**, and **3** on recombinant human brain AChE were kindly provided by Sanochemia Pharmazeutika AG (Wien, Austria).

Chemistry. All solvents, chemicals, and reagents were obtained commercially and used without purification. NMR spectra were obtained at 200 MHz on a Bruker AC-200 FT-NMR spectrometer, with chemical shifts (δ, ppm) reported relative to TMS as an internal standard. Flash chromatography was carried out with Merck silica gel 60 (35−70 μm) using a Shimadzu LC-8A pump and a Shimadzu SPD-6A UV-detector. Purity of target compounds was determined by HPLC using a Waters 2695 instrument with a diode array detector and Merck Chromolith RP_{18} columns and a gradient of 3−60% acetonitrile/water containing 0.1% trifluoroacetic acid at a flow rate of 1 mL/min. The HPLC purity is the number generated for the peak area as calculated using the Water Millenium software with the Maxplot option for the UV maximum of the corresponding peak. Optical rotations were determined using a Perkin-Elmer polarimeter 241.

(4a*S*,6*R*,8a*S*)-4a,5,9,10,11,12-Hexahydro-3-methoxy-11-[3-(1-piperidinyl)propyl]-6*H*-benzofuro[3a,3,2-*ef*][2]benzazepin-6-ol (2). A solution (−)-norgalanthamine[33,34] (0.5 g, 1.83 mM), 0.51 g (3.66 mM) of potassium carbonate, (2.20 mM) of sodium iodide, and *N*-(3-chloropropyl)piperidine (2.20 mM) in acetone (20 mL) were refluxed for three days and concentrated by evaporation. The residue was dissolved in 30 mL of 2N hydrochloric acid and extracted with AcOEt (2 × 20 mL, dicard). The aqueous solution was set at pH > 8.5 with concentrated ammonia and extracted with AcOEt (3 × 20 mL). These extracts were combined, washed with brine, dried (Na_2SO_4), concentrated by evaporation, and purified by flash chromatography using $CHCl_3$/MeOH 97:3 to give 0.73 g (74.7% yield) of the free base; mp 89−92 °C, $\alpha^D_{20} = -50.6°$ (c = 0.25, $CHCl_3$), HPLC 98.5% . ^{1}H NMR (ppm, $CDCl_3$) δ 6.62 (dd, J_1 = 12.6 Hz, J_2 = 8.1 Hz, 2H), 6.08 (d, 12.6 Hz, 1H), 5.98 (dd, J_1 = 8.1 Hz, J_2 = 4.0 Hz, 1H), 4.59 (b, 1H), 4.12 (s, 1H), 4.10 (d, J = 8.1 Hz, 1H), 3.83 (s+d, 4H), 3.33 (t, J = 10.0 Hz, 1H), 3.14 (d, J = 10.0 Hz, 1H), 2.68 (d, J = 10.0 Hz, 1H), 2.35 (m, 9H), 2.01 (m, 2H), 1.68 (q, J = 4 Hz, 2H), 1.60 (m, 3H), 1.48 (m, 3H). ^{13}C NMR (ppm, $CDCl_3$) δ 146.2 (s), 144.4 (s), 133.5 (s),129.8 (s), 127.9 (d), 127.3 (d), 122.4 (d), 111.5 (d), 89.1 (d), 62.4 (d), 58.1 (t), 57.7 (t), 56.2 (q), 55.0 (tt), 51.9 (t), 50.0 (t), 48.8 (s), 33.3 (t), 30.4 (t), 26.2 (tt), 25.2 (t), 324.7 (t).

Preparation of the Dihydrobromide Dihydrate of (2). To a solution of the free base (0.70 g) in dry ethanol (10 mL), a solution of 60% HBr (0.50 mL) in diethyl ether (20 mL) was added and the reaction mixture stirred at 0 °C for 2 h. The precipitate was filtered, washed with diethyl ether (3 × 5 mL), and dried (60 °C/20 mbar) to give 0.85 g (63% yield) of the salt; mp 175−179 °C, HPLC 96.7%. Anal. $C_{24}H_{34}N_2O_3 \cdot 2HBr \cdot 2H_2O$ calcd C 48.33, H 6.76, Br 26.80, N 4.79; found C 48.05, H 6.45, Br 26.30, N 4.55.

2 [6-[(4a*S*,6*R*,8a*S*)-4a,5,9,10-Tetrahydro-6-hydroxy-3-methoxy-6*H*-benzofuro[3a,3,2-*ef*][2]benzazepin-11(12*H*)-yl]hexyl]-1,2-benzisothiazol-3(2*H*)-one 1,1-dioxide (3). 2-(6-Bromohexy1)-1,2-benzisothiazol-3(2*H*)-one-l, l-dioxide,[35] (2.33 g, 7.32 mM), norgalanthamine[33,34] (2.00 g, 7.32 mM), and *N*-ethyldiisopropylamine (2.84 g, 22.0 mM) in absolute chloroform (20 mL) were stirred at boiling temperature for 24 h. The solvent was evaporated and the residue purified by flash chromatography (150 g of silica gel, chloroform:methanol:ammonia 96.5:3:0.5) and the product obtained as free base as colorless foam (2.81 g, 71.4% yield). ^{1}H NMR ($CDCl_3$) δ 8.08−7.72 (m, 4H), 6.68−6.55 (m, 2H), 6.12−5.90 (m, 2H), 4.57 (b, 1H), 4.16−4.01 (m, 2H), 3.82−3.65 (m, 6H), 3.52−3.03 (m, 2H), 2.71−2.28 (m, 3H), 2.10−1.71 (m, 4H), 1.55−1.25 (m, 7H). ^{13}C NMR ($CDCl_3$): 158.8 (s), 145.7 (s), 143.9 (s), 137.6 (s), 134.6 (d), 134.2 (d), 133.1 (s), 129.5 (s), 127.4 (d), 127.3 (s), 126.9 (d), 125.0 (d), 121.9 (d), 120.8 (d), 111.1 (d), 88.6 (d), 62.0 (d), 57.6 (t), 55.8 (q), 51.5 (t), 48.3 (t), 39.3 (t), 32.9 (t), 29.9 (t) 28.2 (t), 27.1 (t), 26.7 (t) 26.6 (t).

Preparation of the Mono Fumarate of (3). A hot solution of the base (1.686 g, 3.13 mM) in EtOH (95%, 10 mL) is combined with saturated solution of fumaric acid (10 mL, about 0.5 M in 95% ethanol) and heated at about 60 °C until a clear solution is obtained. This hot solution is added slowly with magnetic stirring to dry ether (200 mL), resulting in the formation of a precipitate. After standing overnight at room temperature, the solid is filtered, washed with dry ether (3 × 50 mL), and dried at room temperature at 50 mbar over calcium chloride. The fumarate is obtained in the form of a colorless powder (1.560 g, 76% yield). A sample is dried at 2 mbar and at 40 °C for 8 h over phosphorus pentoxide. $\alpha^D_{20} = -61.9°$ (c = 0.39, H_2O). Anal. $C_{29}H_{34}N_2O_6S \cdot C_4H_4O_4$ calcd C 60.54, H 5.85, N 4.28; found C 60.49, H 5.97, N 4.22.

Crystallization. Sanochemia Pharmazeutika AG (Wien, Austria) kindly provided the two galanthamine derivatives. *Tc*AChE was isolated, purified and crystallized as previously described.[36] The crystals of the complexes were obtained by soaking the native crystals at 4 °C in 10 mM inhibitor, 42% PEG200, 100 mM MES at pH 6.0 for 48 h in the case of **2** and 63 h for **3**.

Structure Determination. X-ray diffraction data were collected at the XRD-1 beamline of the Italian Synchrotron Facility ELETTRA (Trieste, Italy). A MarCCD detector (Mar USA, Inc.) and focusing optics were employed for the measurements. The crystals were flash-cooled in a nitrogen stream at 120 K, using an Oxford Cryosystems cooling device (Oxford, UK). Data processing was done with DENZO, SCALEPACK,[37] and the CCP4 package.[38] The enzyme−inhibitor structures were determined by Patterson search methods using the refined coordinates of the native *Tc*AChE,[39] (PDB ID 1EA5)[40] after

Table 1. Summary of Crystallographic Data

	*Tc*AChE-**2**	*Tc*AChE-**3**
Data Collection		
X-ray source	XRD-1 ELETTRA, Trieste (Italy)	
wavelength (Å)	1.00	
detector	MarCCD	
space group	$P3_121$	
unit cell parameters		
a,*b* (Å)	112.19	111.34
c (Å)	137.19	137.21
mosaicity (deg)	0.63	0.42
resolution range (Å)	19.82−2.26 (2.28−2.26)[a]	19.91−2.19 (2.28−2.19)[a]
number of measurements	439740	402326
number of unique reflections ($I \geq 0$)	47210 (957)	50750 (5013)
completeness (%)	99.7 (97.3)	99.6 (99.3)
multiplicity	9.3 (2.9)	8.3 (7.6)
$\langle I/\sigma(I)\rangle$	8.8 (2.0)	10.5 (1.3)
R_{sym}[b]	0.047 (0.418)	0.037 (0.269)
Refinement Statistics		
resolution range (Å)	19.82−2.26	19.91−2.19
number of reflections ($F_o \geq 0$)	46822	50491
R[c]	0.180	0.183
[d] R_{free}	0.212	0.212
number of atoms		
non-hydrogen protein	4263	4245
solvent molecules	398	374
non-hydrogen inhibitor	29	38
non-hydrogen carbohydrate	42	42
rmsd bond lengths/bond angles (Å, deg)[e]	0.011/1.6	0.011/1.6
Ramachandran plot (%) favored/additional allowed/generously allowed/disallowed regions (%)[f]	89.0/10.3/0.4/0.2	89.9/9.5/0.4/0.2
Average Temperature Factors (Å^2)		
protein	39.3	34.9
water	47.6	44.2
inhibitor	40.5	39.7
carbohydrates	63.2	55.4
rmsd ΔB (Å^2)[g]	3.94	3.61

[a] Number in parentheses refer to the highest resolution shell. [b] $R_{sym} = \sum_h\sum_i|I_{h,i} - \langle I_h\rangle|/\sum_h\sum_i I_{h,i}$, with I_h is the *i*th measurement of reflection *h*, and $\langle I_h\rangle$ is the average over symmetry related observation of unique reflection *h*. The summations include all observed reflections. [c] $R = \sum_h|F_o| - |F_c|/\sum_h|F_o|$, where $|F_o|$ and $|F_c|$ are the observed and calculated structure factor amplitudes for reflection *h*. The summation is extended over all unique reflections to the specified resolution. [d] R_{free}, *R* factor calculated using 4701/5088 randomly chosen reflections (10%) set aside from all stages of refinement. [e] Stereochemical criteria are those of Engh and Huber.[48] [f] The catalytic residue Ser200 is in the disallowed allowed region.[49] [g] rmsd ΔB is the rms deviation of the *B* factor of bonded atoms.[50]

removal of the water molecules. Crystallographic refinement of both complexes was performed with CNS version 1.2.[41] In both structures, all data within the resolution range were included with no-σ cutoff. Bulk solvent correction and anisotropic scaling were applied. The Fourier maps were computed with σ-A weighted ($2|F_o| - |F_c|$, Φ_c) and ($|F_o| - |F_c|$, Φ_c) coefficients[42] after initial refinement of the native protein by simulated annealing (at a maximum temperature of 3000 K), followed by maximum likelihood positional and individual isotropic temperature factor refinements. A prominent electron density feature in the catalytic gorge and along the gorge itself in the case of the structure of the complex with **3**, allowed unambiguous fitting of the inhibitors. Carbohydrates (*N*-acetyl β-D-glucosamine linked at Asn59 and Asn416) were built in by inspecting electron density maps. Peaks in the difference Fourier maps that were greater than 2.5σ were automatically added as water molecules to the atomic model and retained if they met stereochemical requirements, and their B factor was less than 70 Å^2 after refinement. Map inspection and model correction during refinement were based on the graphics program O.[43] The crystal parameters, data collection, and refinement statistics are summarized in Table 1. Structure alignments were done using the program LSQMAN.[44] Figures were created using LIGPLOT,[45] PyMOL,[46] and MOE.[47]

References

(1) Perry, E. K.; Tomlinson, B. E.; Blessed, G.; Bergman, K.; Gibson, P. H.; Perry, R. H. Correlation of cholinergic abnormalities with senile plaques and mental test scores in senile dementia. *Br. Med. J.* **1978**, *25*, 1457–1459.

(2) Selkoe, D. J. Biochemistry of altered brain proteins in Alzheimer's disease. *Annu. Rev. Neurosci.* **1989**, *12*, 463–490.

(3) Schrattenholz, A.; Pereira, E. F.; Roth, U.; Weber, K. H.; Albuquerque, E. X.; Maelicke, A. Agonist responses of neuronal nicotinic acetylcholine receptors are potentiated by a novel class of allosterically acting ligands. *Mol. Pharmacol.* **1996**, *49*, 1–6.

(4) Maelicke, A. In *Therapeutic Strategies in Dementia*; Ritchie, C. W., Ames, D., Masters, C. L., Cummings, J., Eds.; Clinical Publishing: Oxford, 2007; pp 153−172

(5) Davis, K. L.; Powchik, P. Tacrine. *Lancet* **1995**, *345*, 625–630.

(6) Kawakami, Y.; Inoue, A.; Kawai, T.; Wakita, M.; Sugimoto, H.; Hopfinger, A. J. The rational for E2020 as a potent acetylcholinesterase inhibitor. *Bioorg. Med. Chem.* **1996**, *4*, 1429–1446.

(7) Enz, A.; Boddeke, H.; Gray, J.; Spiegel, R. Pharmacologic and clinicopharmacologic properties of SDZ ENA 713, a centrally

selective acetylcholinesterase inhibitor. *Ann. N.Y. Acad. Sci.* **1991**, *640*, 272–275.
(8) Marco-Contelles, J.; do Carmo Carreiras, M.; Rodriguez, C.; Villarroya, M.; Garcia, A. G. Synthesis and pharmacology of galantamine. *Chem. Rev.* **2006**, *106*, 116–133.
(9) Liang, P. H.; Ling-Wei Hsin, L. W; Pong, S. L.; Hsu, C. H.; Cheng, C. Y. Synthesis of galanthamine analogs as acetylcholinesterase inhibitors via intramolecular Heck cyclization. *J. Chin. Chem. Soc.* **2003**, *50*, 449–456.
(10) Knesl, P.; Yousefi, B. H.; Mereiter, K.; Jordis, U. Synthesis of (−)- and (+)-8-fluoro-galanthamine. *Tetrahedron Lett.* **2006**, *47*, 5701–5703.
(11) Vanlaer, S.; De Borggraeve, W. M.; Voet, A.; Gielens, C.; De Maeyer, M.; Compernolle, F. Spirocyclic pyridoazepine analogues of galanthamine: synthesis, modeling studies and evaluation as inhibitors of acetylcholinesterase. *Eur. J. Org. Chem.* **2008**, 2571–2581.
(12) Jordis, U.; Froehlich, J.; Treu, M.; Hinschall, M.; Czollner, L.; Kaeltz, B.; Welzig, S. New derivative and analogue of galanthamine. European Patent EP 1 181 294 B1, **2001**.
(13) Herlem, D.; Martin, M. T.; Thal, C.; Guillou, C. Synthesis and structure−activity relationships of open D-ring galanthamine analogues. *Bioorg. Med. Chem. Lett.* **2003**, *13*, 2389–2391.
(14) Guillou, C.; Mary, A.; Renko, D. Z.; Gras, E.; Thal, C. Potent acetylcholinesterase inhibitors: design, synthesis and structure−activity relationships of alkylene linked bis-galanthamine and galanthamine-galanthaminium salts. *Bioorg. Med. Chem. Lett.* **2000**, *10*, 637–639.
(15) Mary, A.; Renko, D. Z.; Guillou, C.; Thal, C. Potent acetylcholinesterase inhibitors: design, synthesis, and structure−activity relationships of bis-interacting ligands in the galanthamine series. *Bioorg. Med. Chem.* **1998**, *6*, 1835–1850.
(16) Pilger, C.; Bartolucci, C.; Lamba, D.; Tropscha, A.; Fels, G. Accurate prediction of the bound conformation of galanthamine in the active site of *Torpedo californica* acetylcholinesterase using molecular docking. *J. Mol. Graphics Modell.* **2001**, *19*, 288–296.
(17) Greenblatt, H. M.; Guillou, C.; Guérard, D.; Argaman, A.; Botti, S.; Badet, B.; Thal, C.; Silman, I.; Sussman, J. L. The complex of a bivalent derivative of galanthamine with *Torpedo* acetylcholinesterase displays drastic deformation of the active site gorge: implication for structure-based drug design. *J. Am. Chem. Soc.* **2004**, *126*, 15405–15411.
(18) Mary, A.; Renko, D. Z.; Guillou, C.; Thal, C. Selective *N*-demethylation of galanthamine to norgalanthamine via a non classical Polonovski reaction. *Tetrahedron Lett.* **1997**, *38*, 5151–5152.
(19) Treu, M.; Hirnschall, M.; Froehlich, J.; Czollner, L.; Kaelz, B.; Kaelz, T.; Kuehnhackl, P.; Jordis, U. Methods for producing norgalanthamine, as well as isomers, salts and hydrates thereof. PCT Int. Appl. WO 2003080623, **2003**.
(20) Commerford, J. D.; Donahoe, H. B. *N*-(ω-Bromoalkyl)saccharins and *N*,*N*′-undecamethylene disaccharin. *J. Org. Chem.* **1956**, *21*, 583–584.
(21) Bartolucci, C.; Perola, E.; Pilger, C.; Fels, G.; Lamba, D. Three dimensional structure of a complex of galanthamine (Nivalin) with acetylcholinesterase from *Torpedo californica*: implications for the design of new anti-Alzheimer drugs. *Proteins* **2001**, *42*, 182–191.
(22) Greenblatt, H. M.; Kryger, G.; Lewis, T. T.; Silman, I.; Sussman, J. L. Structure of acetylcholinesterase complexed with (−)-galanthamine at 2.3A resolution. *FEBS Lett.* **1999**, *463*, 321–326.
(23) Mihailova, D.; Yamboliev, I. Pharmacokinetics of galanthamine hydrobromide (Nivalin) following single intravenous and oral administration in rats. *Pharmacology* **1986**, *32*, 301–306.
(24) Harel, M.; Schalk, I.; Ehret-Sabatier, L.; Bouet, F.; Goeldner, M.; Hirth, C.; Axelsen, P. H.; Silman, I.; Sussmann, J. L. Quaternary ligand binding to aromatic residues in the active-site gorge of acetylcholinesterase. *Proc. Natl. Acad. Sci. U.S.A.* **1993**, *90*, 9031–9035.
(25) Kryger, G.; Silman, I.; Sussmann, J. L. Structure of acetylcholinesterase complexed with E2020 (Aricept): implications for the design of new anti-Alzheimer drugs. *Structure* **1999**, *7*, 297–307.
(26) Bartolucci, C.; Perola, E.; Cellai, L.; Brufani, M.; Lamba, D. "Back door" opening implied by the crystal structure of a carbamoylated acetylcholinesterase. *Biochemistry* **1999**, *38*, 5714–5719.
(27) McMartin, C.; Bohacek, R. S. J. Powerful, rapid computer algorithms for structure-based drug design. *J. Comput.-Aided Mol. Des.* **1997**, *11*, 333–344.
(28) Alisaraie, L.; Haller, L. A.; Fels, G. A QXP-based multistep docking procedure for accurate prediction of protein−ligand complexes. *J. Chem. Inf. Model.* **2006**, *46*, 1174–1187.
(29) Kone, S.; Galland, N.; Graton, J.; Illien, B.; Laurence, C.; Guillou, C.; Le Questel, J. Y. Structural features of neutral and protonated galanthamine: A crystallographic database and computational investigation. *Chem. Phys.* **2006**, *49*, 5051–5058.
(30) Xu, Y.; Colletier, J. P.; Weik, M.; Jiang, H.; Moult, J.; Silman, I.; Sussman, J. L. Flexibility of aromatic residues in the active-site gorge of acetylcholinesterase: X-ray vs molecular dynamics. *Biophys. J.* **2008**, *95*, 2500–2511.
(31) Xu, Y.; Colletier, J. P.; Jiang, H.; Silman, I.; Sussman, J. L.; Weik, M. Induced-fit or pre-existing equilibrium dynamics? Lessons from protein crystallography and MD simulations on acetylcholinesterase. *Protein Sci.* **2008**, *17*, 601–605.
(32) Ravelli, R. B. G.; Raves, M. L.; Ren, Z.; Bourgeois, D.; Roth, M.; Kroon, J.; Silman, I.; Sussman, J. L. Static Laue diffraction studies on acetylcholinesterase. *Acta Crystallogr., Sect. D: Biol. Crystallogr.* **1998**, *54*, 1359–1366.
(33) Mary, A.; Renko, D. Z.; Guillou, C.; Thal, C. Selective *N*-demethylation of galanthamine to norgalanthamine via a non-classical Polonovski reaction. *Tetrahedron Lett.* **1997**, *38*, 5151–5152.
(34) Treu, M.; Hirnschall, M.; Froehlich, J.; Czollner, L.; Kaelz, B.; Kaelz, T.; Kuehnhackl, P.; Jordis, U. Methods for producing norgalanthamine, as well as isomers, salts and hydrates thereof. PCT Int. Appl. WO 2003080623, **2003**.
(35) Commerford, J. D.; Donahoe, H. B. *N*-(ω-Bromoalkyl)saccharins and *N*,*N*′-undecamethylene disaccharin. *J. Org. Chem.* **1956**, *21*, 583–584.
(36) Sussman, J. L.; Harel, M.; Frolow, F.; Varon, L.; Toker, L.; Futerman, A. H.; Silman, I. Purification and crystallization of a dimeric form of acetylcholinesterase from *Torpedo californica* subsequent to solubilization with phosphatidylinositol-specific phospholipase C. *J. Mol. Biol.* **1988**, *203*, 821–823.
(37) Otwinowski, Z.; Minor, W. Processing of X-ray diffraction data collected in oscillation mode. *Methods Enzymol.* **1997**, *276*, 307–326.
(38) Collaborative Computational Project No. 4. *Acta Crystallogr., Sect D: Biol. Crystallogr.*, **1994**, *50*, 760−763.
(39) Sussmann, J. L.; Harel, M.; Frolow, F.; Oefner, C.; Goldman, A.; Toker, L.; Silman, I. Atomic structure of acetylcholinesterase from *Torpedo californica*: a prototypic acetylcholine-binding protein. *Science* **1991**, *253*, 872–879.
(40) Dvir, H.; Jiang, H. L.; Wong, D. M.; Harel, M.; Chetrit, M.; He, X. C.; Jin, G. Y.; Yu, G. L.; Tang, X. C.; Silman, I.; Bai, D. L.; Sussman, J. L. X-Ray structures of *Torpedo californica* acetylcholinesterase complexed with (+)-Huperzine A and (−)-Huperzine B: structural evidence for an active site rearrangement. *Biochemistry* **2002**, *41*, 10810–10818.
(41) Brünger, A. T.; Adams, P. D.; Clore, G. M.; DeLano, W. L.; Gros, P.; Grosse-Kunstleve, R. W.; Jiang, J. S.; Kuszewski, J.; Nigels, M.; Pannu, N. S.; Read, R. J.; Rice, L. M.; Simonson, T.; Warren, G. L. Crystallography & NMR system: a new software suite for macromolecular structure determination. *Acta Crystallogr., Sect. D: Biol. Crystallogr.* **1998**, *54*, 905–921.
(42) Read, R. J. Improved Fourier coefficients for maps using phases from partial structures with errors. *Acta Crystallogr., Sect. A: Found. Crystallogr.* **1986**, *42*, 140–149.
(43) Jones, T. A.; Zou, J. Y.; Cowan, S. W.; Kjeldgaard, M. Improved methods for building protein models in electron density maps and the location of errors in these models. *Acta Crystallogr., Sect. A: Found. Crystallogr.* **1991**, *47*, 110–119.
(44) Kleywegt, G. J. Use of non-crystallographic symmetry in protein structure refinement. *Acta Crystallogr., Sect. D: Biol. Crystallogr.* **1996**, *52*, 842–857.
(45) Wallace, A. C.; Laskowski, R. A.; Thornton, J. M. *LIGPLOT*: a program to generate schematic diagrams of protein-ligand interactions. *Protein Eng.* **1995**, *8*, 127–134.
(46) DeLano, W. L. *The PyMOL Molecular Graphics System*; DeLano Scientific LLC: San Carlos, CA, http://www.pymol.org.
(47) *Molecular Operating Environment* (*MOE 2008.10*); Chemical Computing Group, Inc.: 1010 Sherbrooke St. W, Suite 910 Montreal, Quebec, Canada H3A 2R7.
(48) Engh, R. A.; Huber, R. Accurate bond and angle parameters for X-ray protein structure refinement. *Acta Crystallogr., Sect. A: Found. Crystallogr.* **1991**, *47*, 392–400.
(49) Laskowski, R. A.; MacArthur, M. W.; Moss, D. S.; Thornton, J. M. PROCHECK: a program to check the stereochemical quality of protein structures. *J. Appl. Crystallogr.* **1993**, *26*, 283–291.
(50) Kleywegt, G. J. Validation of protein models from Cα coordinates alone. *J. Mol. Biol.* **1997**, *273*, 371–376.